Design and Testing of LEDSOL Components for Sustainable Access to Clean Water in Africa

Elena Simona Lohan, Xiaolong Zhang, Tampere University, Tampere, Finland name.surname@tuni.fi

Tomkouani Kodom University of Lomé, Lomé, Togo tomkouani.kodom@gmail.com

Oana Cramariuc[1], Irina Mocanu[1], Iulian Năstac[2] CITST[1]/UPB[2], Bucharest, Romania {name.surname}@citst.ro

Hafida Lebik[3], Rafik Elhadi[4] UDES[3]/CRAPC[4], Alger, Algeria h.lebik@udes.dz rafikelhadi591@gmail.com

***Abstract*—Access to potable water is still a challenge in many African regions. Our transnational project, LEDSOL, aims at enabling a sustainable access to clean water through a combination of three components: a smart UV/LED disinfection unit, a solar-energy-based power source, and a standalone low-cost satellite-based positioning engine. This paper presents the first unified set of test results based on the three individual components of LEDSOL system and discusses further challenges. Water quality measurements from Togo and Algeria are also presented to illustrate the severity of the problem.**

I. Introduction

Access to potable water is a fundamental need of humankind; yet, this access is still challenging in several parts of the world due to several factors, such as scarce water availability in arid regions, water pollution or contamination with different parasites and bacteria, mismanagement of water resources, natural disasters affecting water infrastructures, poor infrastructures to access the potable water sources, etc. [1], [2]. Based on UN-Water facts and report [3], two billion people in the world did not have access in 2020 to "safely managed drinking water services" and between 1.7 and 2.4 billion people in the world are likely to experiment water scarcity by 2050, which makes the sustainable access to clean water a top priority goal in research and innovation endeavours worldwide. The Long-Term Joint European Union - African Union Research and Innovation Partnership on Renewable Energy (LEAP-RE)[1] is one of the many research and innovation initiatives focusing on renewable and sustainable access to various fundamental resources, from energy to water and food. Our LEDSOL project[2] ("Enabling clean and sustainable water through smart UV/LED disinfection and SOLar energy utilization") is a part of the LEAP-RE initiative and focuses on three main axes related to sustainable solutions for access to clean and potable water [4]:

- Providing a new architecture and design for a LED/UV-based portable water disinfection unit;
- Proposing a novel standalone low-cost satellite-based positioning engine for the portable solution, to serve in a variety of situations, such as: mapping the water sources and optimizing the access paths to them, monitoring the water distribution infrastructures based on location information, helping in real-time tracking and distribution of portable units, aiding in emergency responses when water infrastructure has been affected, etc.;
- Designing a solar-powered energy module to sustainably feed the UV/LED disinfection unit and the positioning engine for hours (up to 24h) in a row.

The LEDSOL project is a three-year project who has started in April 2022 and, by the end of it, we expect to have developped a full-chain architecture comprised of the three above-mentioned axes and to be able to test the individual components in several pilot studies in Africa and Europe. It is to be mentioned that the project does not aim at an integrative solution that could be commercialized immediately at its end, but will rather focus on designing novel aspects, algorithms and architectures in each of its three axes.

The goal of this paper is to present the initial set of results in each of the three above-mentioned directions, reminded in Section II: LED/UV-based unit design and testing (addressed in Section IV), the positioning system design and testing (addressed in Section V), and the solar-powered energy unit (addressed in Section VI). Also, real-field ground and surface water measurements from Togo and Algeria are shown in Section III as examples in order to illustrate better the current challenges of the access to potable water in Africa. Conclusions and further steps are given in Section VII.

II. Overall system design

The three system components of the LEDSOL system are illustrated in Fig. 1: a solar-energy module will provide the battery power for the water purification and disinfection unit as well as for the standalone positioning engine. All these three components are to be packed first in a backpack and, subsequently, in a head basket; based on our previous user surveys in Togo [4], it was seen that a head basket is preferable to a backpack solutions in Africa, as typically the women are those expected to carry the water (and the associated water-purification system) and their backs are usually occupied with carrying their babies. The main challenges identified so far are multiple [4]:

- The overall system weight should not surpass 25 Kg, which could limit the water reservoir capacity and would

[1]https://www.leap-re.eu/
[2]https://www.leap-re.eu/ledsol/

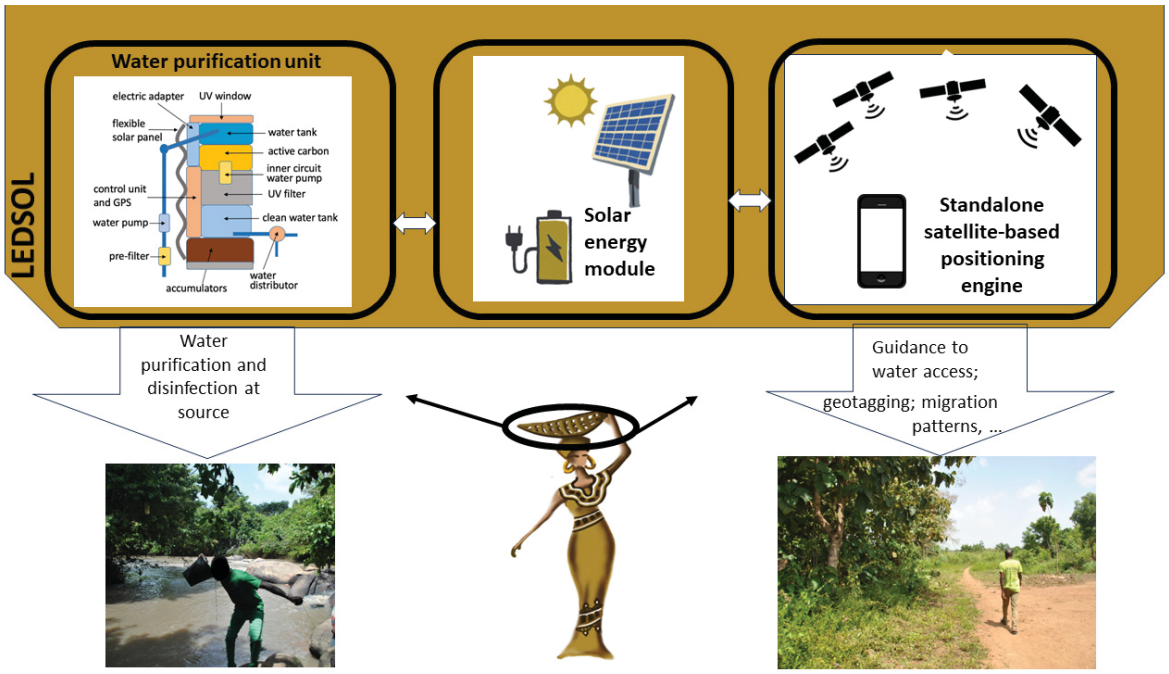

Fig. 1. LEDSOL overall architecture for sustainable access to clean water

impose constraints on the LED/UV efficacy, as well as on the solar cells and accumulators;

- The solar energy module should be able to power on the whole system for several hours in a row, preferably for a full day at a time; currently, we are looking for solutions that would have close to 48h battery autonomy;
- The positioning engine should operate in a standalone mode, assuming viable operations also where there is no access to Wifi or cellular networks; this is currently possible outdoors with the help of Global Navigation Satellite Systems (GNSS), therefore GNSS-based navigation is the focus of our research;
- The system should be affordable and easy to use, which adds the constraints of low cost and low complexity of all the elements of the LEDSOL system.

The next section III presents our recent water-quality measurements conducted in Togo and discusses the relationship between the water quality variables and the potential contamination sources. Sections IV, V, and VI detail our testing results so far, component by component.

III. Water Quality Measurements

Four campaigns for water measurements have been conducted in Togo and Algeria at the following four locations (the measurement date is shown in brackets): a) surface water (SW) - sample from river Haho, Togo (26.09.2023); b) Ground Water (GW) - sample from a well in Agoe-Zongo, Togo (29.08.2023); c) water source in Aïn Bahloul - Aïn Tagouraït, Algeria (21.03.2023); and d) water source in Sidi Bouzid - Kolea, Algeria (21.03.2023). The measurement equipment were different in Togo and Algeria, but all focused on measuring the physico-chemical and bacterial properties of the water sources. In Togo, an extensive study of minerals in the water was performed, while this study was not done in Algeria, thus some of the values will appear as N/A (not available). In Togo, the water samples were collected in polyethylene terephthalate (PET) 1.5-liter bottles for physico-chemical analysis, while 0.5-liter sterilized bottles were used for bacteriological analysis. The selected physico-chemical and bacteriological parameters were determined according to AFNOR (Association Française de Normalisation) standard [5], [6]. To assess the groundwater suitability for drinking and domestic purposes, the hydro-chemical and microbiological results were compared to WHO water quality standards [7]. The principal Component Analysis (PCA) was performed using Statistica software. The water quality measurements in Algeria were done with the help of the Algerian Ministry of Irrigation. Initially, 218 water sources were prospected, and two of them were selected (Aïn Bahloul - Aïn Tagouraït and Sidi Bouzid - Kolea) for further detailed measurements as being representative enough for a wider environment. The physico-chemical and bacteriological characteristics of the analyzed water samples are shown in Table I. SW stands for Surface Water, GW stands for Ground water, CFU stands for colony forming units, EC stands for the electrical conductivity, TDS stands for Total Dissolved Solids, and NTU stands for Nephelometric Turbidity units.

As seen in Table I, in Togo, the salinity or mineralization is high for groundwater (EC$>$ 1000) while it has a low-to-middle value (20 $<$EC$<$ 333) for surface water; in Algeria the salinity is high at both locations. Also, bacteriological characteristics of the analyzed water samples do not satisfy, most of the times,

TABLE I. MEASURED WATER QUALITY IN FOUR LOCATIONS IN TOGO AND ALGERIA; RED VALUES SHOW ABNORMAL LEVELS

Parameter	**River Haho SW, Togo)**	**Agoe-Zongo GW, Togo**	**Aïn Tagouraït GW, Algeria**	**Kolea GW, Algeria**	**Maximum value (WHO/EU standards) [7]**
Date	**26.09.2023**	**29.08.2023**	**21.03.2023**	**21.03.2023**	
Total coliformes [UFC/250 ml]	60	200	375	375	1
Escherichia coli [UFC/250 ml]	N/A	N/A	375	5	0
Faecal Streptococi [UFC/250 ml]	10	120	7.5	0	1
pH	7.9	7.4	8.1	6.8	6.5 – 8.5
Temperature [^{o}C]	26.7	27	20.6	22.5 C	–
EC [µs/cm]	320	1130	1760	1270	400
TDS [mg/l]	253	856	940	670	1500
Turbidity [NTU]	20.2	2.2	N/A	N/A	5
Sodium [mg/L]	20	128	N/A	N/A	150
Potassium [mg/L]	3	20.8	N/A	N/A	12
Magnesium [mg/L]	0	0.4	N/A	N/A	0.5
Total Iron [mg/L]	0.6	0	N/A	N/A	0.3

the WHO criteria [7] showing that the water quality is often not enough for drinking purposes.

The Togo data has been analyzed in more detail also via Statistica software. We have observed that the surface water is characterized by low mineralization, as indicated by the electrical-conductivity value and by a low content of minerals. However, it is to be noticed that a high turbidity (i.e., low water clarity) is observed due to the runoff water and to the high flow regime of Haho river. This high turbidity can explain well the high microorganism content of this water. Indeed, from a microbiological point of view, this SW water is high polluted and unsuitable for drinking purpose. The other analyzed water source, the GW from a well in Agoé-Zongo in Togo showed a high mineral content with EC about 1130 µs/cm and a high potassium content, above WHO standards limits. A high mineralization of shallow groundwater in larger Lomé area was also reported in 2020 by Akpataku et al. [8]. A Principal Component Analysis (PCA) based on the correlation matrix was performed to understand the underlying relationships between the water quality variables and the potential contamination sources. Fig. 2 shows the biplot of the PCA of the physico-chemical data of the two water samples taken in Togo (SW and GW water samples). The strongest-feature factors, called F1 and F2, account to 90.75% of the total variance, leading to a good-enough interpretation based on only these two factors. The European (EU) and WHO standards are also shown in Fig. 2, for a good comparison with SW and GW samples and they show a poor quality of SW and GW water. As seen in Fig. 2, there is a higher proximity

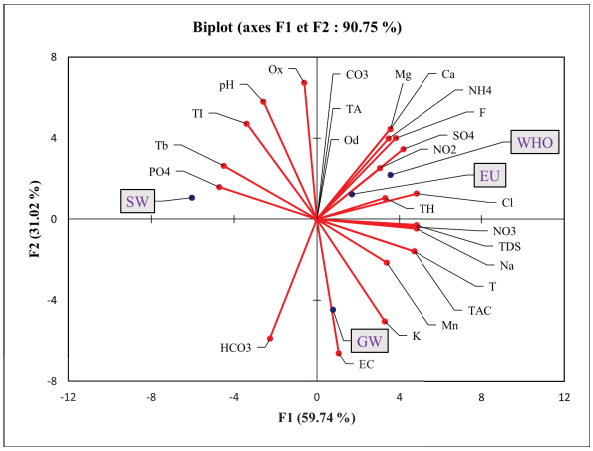

Fig. 2. Principal Component Analysis (PCA) of chemical data showing correlation between the different analyzed vari-ables (SW: surface water, GW: groundwater)

between ground water parameter and the EU standards than between the SW water and EU standard. The situation in Fig. 2 also shows that ground water is under anthropic influence and that this area is characterized by high unsanitary condition that could quickly affect the water quality. The bacteriological analysis has also revealed this contamination and then the consumption of these waters is a critical health risk especially to children, therefore water purification and disinfection is

of utmost importance. The next section details the steps and testing results so far we have undertaken for a LED/UV-based water disinfection unit.

IV. LED/UV DESIGN AND TESTING

A. Design of the disinfection unit

The design of the UV/LED water disinfection unit is generally defined by the initial requirements set for the system, either due to technological constrains or by our target performance. As such, the water disinfection unit should have a low energy consumption, should work in continuous flow and in direct current (DC) mode to avoid energy losses due to conversion and ensure up to 2 l/min disinfected water. This poses constraints on the water pump which is fueling the UV/LED disinfection chamber, LEDs, and the chamber itself. In addition, the first prototypes should be tested under laboratory conditions and allow for aggressive cleaning after each testing cycle such that no cross-contamination takes place between tests. The design of our treatment chamber is presented in Fig. 3. The chamber is made out of Teflon and its dimensions were calculated based on estimates of the required radiation power and on the water flow rate.

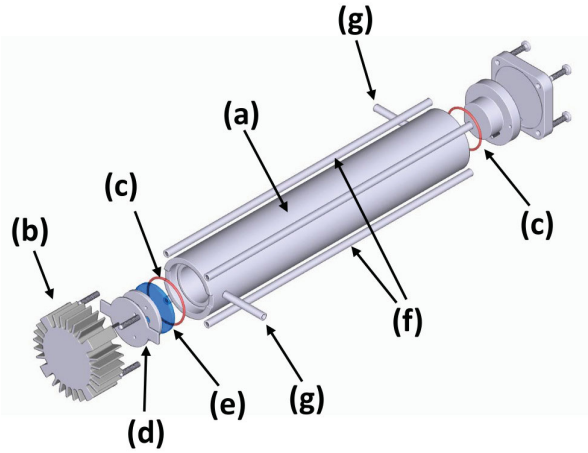

Fig. 3. Treatment chamber comprising: (a) Teflon tube 25cm in length, inner and outer diameter 3 and 5 cm, respectively;(b) Aluminium radiators; (c) gskets; (d) PCB with LEDs; (e) quartz window; (f) fastening systems; (g) water flow pipes.

We remind the reader that the ultraviolet (UV) LEDs are of three categories, based on their wavelength: UV-A (between 320 and 400 nm wavelength), UV-B (280–315nm), and UV-C (200–280nm) ranges. The selected LEDs are Osram SU CULDN1 types, and in particular the VC-OSRAM type for the UV-C radiation[3] and the KTDS-3534UV365B-KINGBRIGT type for the UV-A radiation[4]. The UV-C LEDs were selected such as to also partially emit in the UV-B domain, thus covering the entire wavelength spectrum needed for disinfection. Our prototype comprises two UV-C LEDs connected in series and one UV-A LED. The LEDs are mounted on a custom designed PCB and cooled via aluminum radiators. For the UV disinfection to be effective, the water must be without impurities, so that it has good radiation transparency. Additionally, this is also needed to meet the requirements for drinking water. For this purpose, mechanical filters will be used, which will be installed both upstream of the pump supplying water from the surface source and along the internal water circuit. Two pumps will be used to pump the water. One of the pumps will pump water from the surface source (e.g., lake, spring) into the backpack. The second pump will pump water through the backpack circuit. Based on an extensive survey of available pumps we have selected the DAYPOWER WP-165 as the first pump and the AC060210-4890 as the second pump. Both pumps were purchased from Pollin, operate in DC and their theoretical flow is able to deliver at least double of the targeted 2 l/min. In addition, laboratory tests require a pump which can withstand aggressive chemical cleaning after each testing cycle. We have selected a M1500 series peristaltic pump from Verder Liquids. Some of the pumps are fitted with motors which are capable to reach more rotations per minute than the original ones. In this way we are able to pump 2 l/min of water. The disinfection laboratory prototype which incorporates two glass reservoirs, the treatment chamber, a peristaltic pump and a flow meter is shown in Fig. 4.

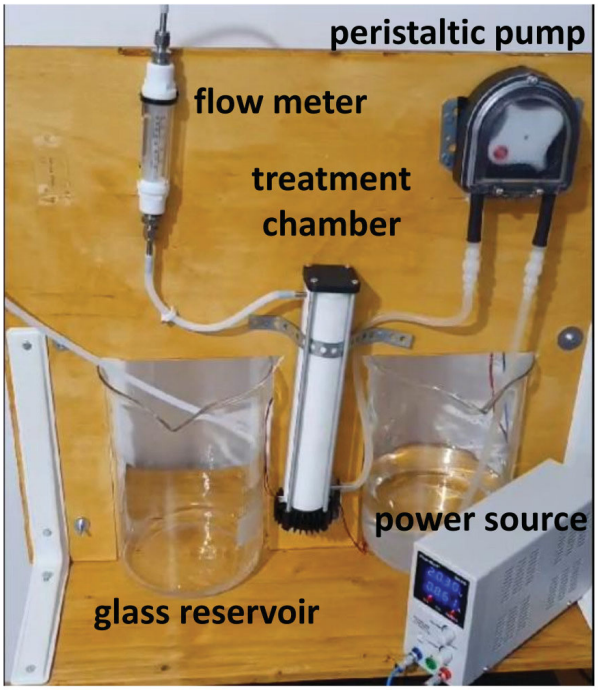

Fig. 4. LEDSOL disinfection laboratory prototype based on UV/LED irradiation

[3]https://dammedia.osram.info/media/resource/hires/osram-dam-17966695/SU\%20CULDN1.VCEN.pdf

[4]https://www.ttieurope.com/content/dam/tti-europe/manufacturers/kingbright/resources/KTDS-3534UV365B(Ver.1B).pdf

B. Testing of the UV/LED component

In order to determine the intrinsic power output of the LEDs, we used a Thorlabs S405C thermal power sensor head (TPSH) connected to a PC. The TPSH has a 10 mm diameter sensitive surface, can be used in the spectral range of 0.19 to 20 µm and allows for measurements of powers from 100 µW up to 5 W. We performed measurements at distances of 2, 4 and 6 cm from the surface of the LEDs holder to the front surface of the TPSH both for the UV-A LED and the two UV-C LEDs, the latter either separately or in series configuration. The measurements were also performed with and without a quartz window positioned in front of the LEDs. The applied voltage was in the range 3.15 to 6 V for the UV-A LED and 10.85 to 11.57 V for the series connected UV-C LEDs. This resulted in currents in the range 10 to 500 mA for the UV-A LED and 175 to 350 mA for the UV-C LEDs. Our results reveal that the quartz window, when placed on top of the LEDs, does not attenuate the UV power significantly. The attenuation is below 8% at both 365 nm (UV-A) and 275 nm (UV-C). Besides, the relative change in UV power as a function of driving current and distance were assessed and found to be in good agreement with the data given by the manufacturers.

In order to estimate the performance of the LEDs when placed inside the treatment chamber, we measured the UV dose delivered at different locations by means of colorimetric UV-C dosimeters[5]. The sensitive region of such dosimeters changes color depending upon the amount of incident UV energy density. The dosimeters are calibrated at wavelengths between 260 and 280 nm and offer the possibility to compare the color of the sensitive region with colors corresponding to 25, 50, and 100 mJ/cm^2 respectively. Small pieces of the sensitive area of such dosimeters have been placed along the chamber's sidewall at 1, 10, and 24 cm from the fused silica window. Irradiation was performed for 2, 10 and 100 s respectively with the UV-C LEDs alone at a current of 350 mA. While at 1 cm distance 100 mJ/cm^2 are almost achieved after 2 s at larger distances this is not the case. At 24 cm distance 100 s are needed for a energy density of about 25 mJ/cm^2. Thus, a quite large drop in irradiation level has been observed. However, the level of irradiation experienced by a germ inside the chamber is higher, because of photons propagating from basically all directions towards its surface. Thus, tests with reference germs such as Escherichia coli are needed for a definitive assessment of the prototype's performance.

V. Positioning system design and testing

A. Adopted methodology

The methodology we adopted for the positioning studies is illustrated in Fig. 5. Initially, a market review was done to investigate the available devices to conduct raw GNSS measurements. As Android has opened the access to raw GNSS measurements since 2016 [9], Android mobile phones have been a logical choice. After that, another study investigated the different Android apps that collect and store the raw GNSS measurements in various formats (e.g., CSV, RINEX, NMEA benchmarks, etc.). A brief survey of the most relevant Android apps is shown in Table II. ESA apps such as [10], [11] are currently not widely used by the research community to our best knowledge. Based on our survey, we found out that the GNSSLogger app is currently the most mature one and most fit-to-purpose app to store GNSS raw measurements, together with reference tracks in NMEA format (latitude, longitude,altitude). A detailed comparison between GEO++RINEX and GNSSLogger apps can also be found in [12]; the authors in [12] have also concluded that there are less inconsistencies in GNSSLogger recordings than in GEO++RINEX, and that both apps need further improvements. One of such endeavours is our MIMIR app which is now available on GitHub and undergoes further enhancements [13]; it is to be noticed that this app was not available in March 2023 when we started the GNSS measurements in Togo, therefore, for consistency, all measurements analyzed in here were collected via GNSSLogger app.

Therefore, the Android measurements in dynamic conditions (see Fig. 5) have been stored via GNSSLogger app. These measurements include, as also shown in Fig. 5, the RINEX observations (e.g., code and carrier phases from all available GNSS satellites on sky and from all supported frequency bands by the GNSS chipset, carrier-to-noise ratio estimates per visible satellite) and the NMEA reference tracks computed with the proprietary algorithms available on the mobile device; most likely, these proprietary algorithms are likely to integrate also the available sensor data (accelerometer, gyroscopes, etc.) as well as the cellular data and therefore are expected to provide a higher accuracy position estimate than the raw GNSS observables; for this reason and because accurate absolute reference tracks are difficult to achieve in dynamic conditions and require access to expensive professional GNSS receivers, we have taken the NMEA tracks as the reference tracks in our comparative analysis. The broadcast ephemeris (BE) data mentioned in Fig. 5 (i.e., the data that allows the computation of the satellite positions on the sky at the time of the measurements) has been taken from an external server, the IGS server[6]; in theory, some Android devices allow also the access to the BE data, but in practice there is no Android app yet which can store this data; nevertheless, the BE data is exactly the same no matter its origin (directly from the Android device or from the IGS server) and therefore its origin does not affect our subsequent analysis. The analysis, as illustrated in Fig. 5, was done with own in-house developped Matlab software; it is to be noticed that currently, there exists couple of other software tools in open access on Github (including a Matlab GPS software package) that claim to work with GNSSLogger data, but none of them were found suitable for our purpose; therefore, we developped own software to perform the data analysis presented in the next subsection.

[5]https://uvcdosimeters.com/uvc-led-tri-card/

[6]https://igs.bkg.bund.de/root_ftp/IGS/BRDC/

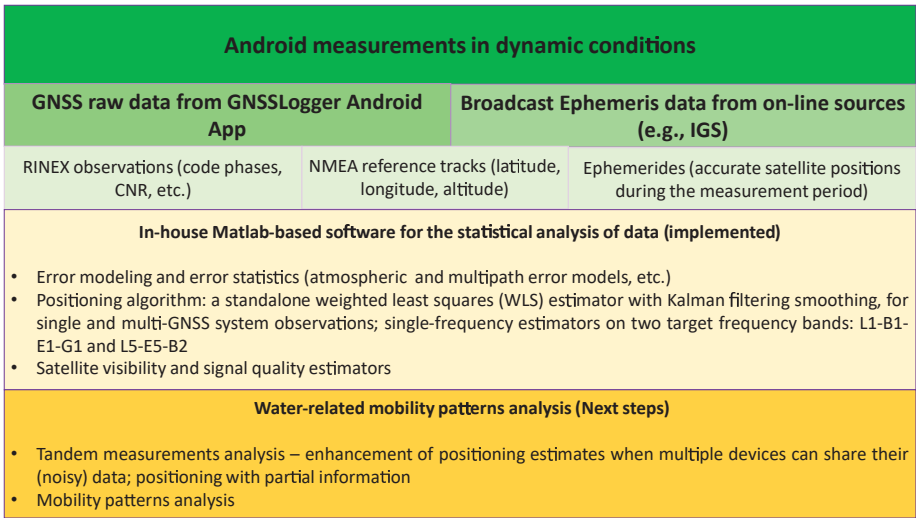

Fig. 5. Measurement-based methodology in positioning studies

TABLE II. COMPARISON OF VARIOUS ANDROID APPS FOR GNSS RAW DATA COLLECTION

App name	Main features	Limitations	Reference
Camaliot	An ESA app saving raw data in CSV format; it support multi-GNSS systems	Access to full features requires login	[11]
Galileo PVT	Another ESA app saving raw data in CSV and RINEX formats	It currently supports only GPS ans Galileo	[10]
GEO++RINEX	App developped by GEO++; the data from multi-GNSS multi-frequency receivers is available in RINEX format; data is saved in two data folders: best observations and full observations	No NMEA reference data;	[14]
GNSS/IMU Logger	An app developped by ISTA-UniBwM to record GNSS and sensor data in RINEX and CSV formats	Not supported anymore on new Android versions; Glonass system not supported	[15]
GNSSLogger	Google app saving multi-GNSS multi-frequency data in CSV, RINEX, and NMEA formats; it has a user-friendly interface and includes several visualization tools	RINEX -formatted data has more inconsistencies than CSV-formatted data	[16]
MIMIR	An app developped in our unit at TAU, available in open source; it provides multi-GNSS and sensor data in CSV formats	No RINEX format available yet; app is still being developped; not available on Google Play	[13]

B. Measurement campaigns description

All measurements have been conducted in dynamic conditions (walk or car), by several volunteers with own Android mobile devices. The measurements were conducted during the period 10th of March - 27th of August 2023, following an informed consent process. Six Android devices were used in the measurements: an Itel w6501 phone, a Moto E6 play phone, a Tecno Spark 7 phone, a Tecno Camon 16 pro phone, an Infinix Hot 6 phone and an Infinix Hot 12i phone; most (if not all) are using Mediatek chipset for the GNSS positioning based on their specification sheets (for few models, such specification sheets were not available). One of the first things we noticed was that Galileo raw data was not available via GNSSLogger on any of the six mobile phones used for testing; most cases gave access to GPS and GLONASS data and sometimes also to Beidou data (more details provided in Table IV); as we only looked as the RINEX data stored by GNSSLogger, it is yet unclear whether the absence of Galileo data is due to some limitations in the RINEX data (e.g., some flags to avoid too much data being stored) or to some shortcomings of GNSSLogger app; further investigations, looking also at the *csv data is necessary; however, the *csv data are huge (of the order of few hundreds of Mb per measurement) and were not transferred at the time of our study.

The next section provides two types of data analysis:

- a scenario-level analysis when two measurements per-

formed during the summer of 2023 are compared in terms of average visibility per satellite and Dilution of Precision (DOP) metrics, namely Horizontal DOP (HDOP), Geometrical DOP (GDOP), Position DOP (PDOP), Vertical DOP (VDOP) and Time DOP (DDOP). As DOP measures (all unitless) are typical performance measures in GNSS, the interested reader is referred to [17] for the mathematical definitions of these expressions. Also comparative bar plots for the Carrier-to-Noise Ratios (CNR) and average satellite elevations during the measurement duration are provided for the scenario-level analysis;

- A conglomerate-level analysis; in here the measurement results collected with the six Android devices are compared in terms of visible GNSS satellites, estimated ionospheric and tropospheric delays τ_{iono} and τ_{tropo} shown, for convenience, in meters, other delays τ_{other}, including for example the hardware and multipath delays, best combination of GNSS systems providing the highest accuracy, as well as the accuracy metrics: the mean and standard deviation of the 2D (horizontal) positioning error: ϵ_{2DMean} and ϵ_{2Dstd}, respectively and the mean and standard deviation of the altitude (or z-direction) estimate: $\epsilon_{z,Mean}$ and $\epsilon_{z,std}$, respectively.

C. Measurements analysis

1) Scenario-level analysis: A first analysis compared two measurement scenarios, one taken on 24th of August 2023 via a Tecno Spark 7 phone and the second one taken on 27th of August via an Infinix Hot 6 phone. An example of the measured track during 27th of August 2023 with the Infinix Hot 6 phone is illustrated in Fig. 6. The dynamic measurements were done in dynamic (walking or driving) conditions.

The scenario-level comparative results are shown in Fig. 7 (CNR comparison), Fig. 8 (satellite elevations), Fig. 9 (atmospheric and multipath error distribution), and Table III (visibility and DOP comparison).

We noticed that the number of satellites per system is a around 10 (with 22 in total visible for two GNSS systems and 32 in total visible for two GNSS systems) and that the Infinix Hot 6 phone stored also the Beidou data in addition to GPS and Glonass data stored by Tecno Spark 7. It is to be remarked that the absence of Galileo satellites does not mean that Galileo satellites are not visible in Togo; it only means that the mobile devices we had available for testing were unable to store the Galileo raw data with the GNSSLogger app. Based on Table III, we can also notice slightly better DOP values for the Infinix Hot 6 phone than for the Tecno Spark 7 phone, which is not surprising being given the extra Beidou system which was available as raw data. Nevertheless, as seen in Fig. 7, the average CNR values are slightly better on the Tecno Spark 7 phone than on the Infinix Hot 6 phone, though with a higher standard deviation. The average satellite elevations are similar as predicted on both phones (see Fig. 8), which is again as expected, and the error distribution (Fig. 9) shows very similar tropospheric errors on average, slightly higher estimates for the ionopsheric errors for the Infinix Hot 6 phone, but much lower other errors, on average, on Infinix Hot 6 phone than on Tecno Spark 7 phone, which will be reflected, as shown later in Table IV, in lower positioning errors with the raw data collected by the Infinix Hot 6 phone than the one collected with the Tecno Spark 7 phone.

2) Conglomerate-level analysis: Table IV shows the conglomerate results from all the measurements we conducted with six different smartphones in Togo during march -August 2023. The duration of each measurement is given in hours, via the T_{obs} (observation time) parameter. The N_{sat} is the average number of observed satellites per GNSS system. The estimated ionopspheric, tropospheric and other delays are denoted via τ_{iono}, τ_{tropo} and τ_{other} and c denotes the light speed. Based on one, two or three visible GNSS systems on a mobile device, we also tested up to 7 combinations of systems in standalone positioning (e.g., GPS, Glonass, GPS+Glonass, GPS+Glonass+Beidou, etc.) in order to find out the best combination in terms of positioning accuracy; unsurprisingly, using all available systems has always proved to give the best accuracy.

Based on Table IV, we can see that reasonable horizontal accuracy (of few meters) can be attainable in most scenarios with Android-quality raw GNSS data (with the exception of the Moto E6 play device that, for some unexplained reason, was able to store only the Glonass raw data, which is the noisiest among the other GNSS systems). We can also see from Table IV a good match between the estimated tropospheric delays, as well as good agreement between the ionospheric delays estimated with data from different phones (with the exception of Tecno Spark 7 phone which seems to underestimate the ionospheric delays on both GPS and Glonass and therefore it has higher residual errors than with the other devices). The vertical positioning accuracy is however rather low with all devices in standalone positioning and it is a part that needs further enhancements.

VI. Solar-powered system design and testing

The LEDSOL overall system is aiming at finding sustainable solutions for water, energy, and positioning at a same time, which is a challenging target. Designing an effective photovoltaic (PV) as a single source of energy for both the water disinfection and positioning engines depends on a variety of factors, including the geographical situation, the meteorological conditions, the technical characteristics of each component and the required power load. In the case of a standalone system, as envisaged by us, the complexity is even greater, since the developed prototype should meet the on-site user's demands. Moreover, as the system is portable, the total weight and dimensions of the PV system components (battery, charge controller and PV module) are important parameters to consider, along with user safety.

A. Architecture and components

The first step for an optimal PV design has been the determination of the load profile. The following four components,

Fig. 6. Example of one measurement track in Togo during our measurement campaigns

TABLE III. COMPARATIVE PERFORMANCE METRICS FOR SCENARIO-LEVEL ANALYSIS. GP=GPS; GL=Glonass; BD=Beidou.

Parameter	**Tecno Spark 7 phone 24.08.2023**	**Infinix Hot 6 phone 27.08.2023**
Total number of visible satellites	22	32
Visible systems	GP+GL	GP+GL+BD
Average visibility/satellite [%]	74.96	81.28
Average GDOP [-]	1.69	1.07
Average PDOP [-]	1.50	0.94
Average HDOP [-]	1.42	0.88
Average VDOP [-]	0.47	0.32
Average TDOP [-]	0.77	0.50

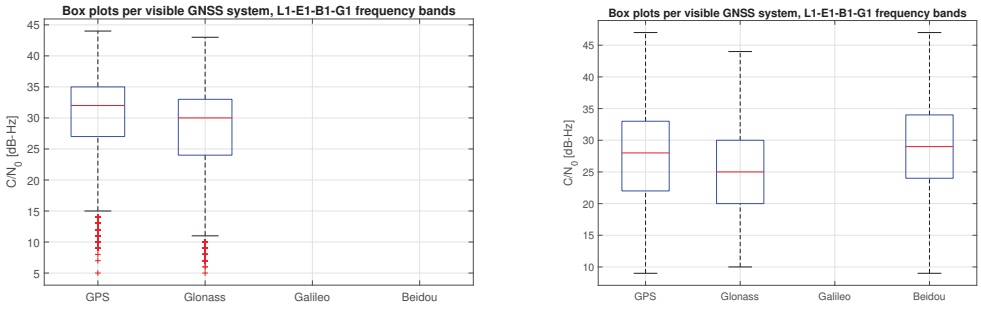

Fig. 7. Distribution of satellite carrier-to-noise ratio (CNR) per GNSS system: a) Tecno Spark 7 phone (only GPS and Glonass satellites visible); b) Infinix Hot 6 phone (GPS, Glonass, and Beidou satellites visible)

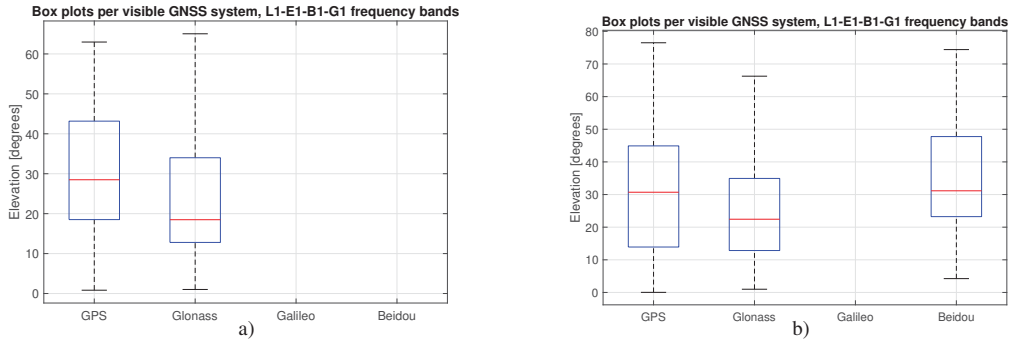

Fig. 8. Distribution of satellite elevations per GNSS system: a) Tecno Spark 7 phone (only GPS and Glonass satellites visible); b) Infinix Hot 6 phone (GPS, Glonass, and Beidou satellites visible)

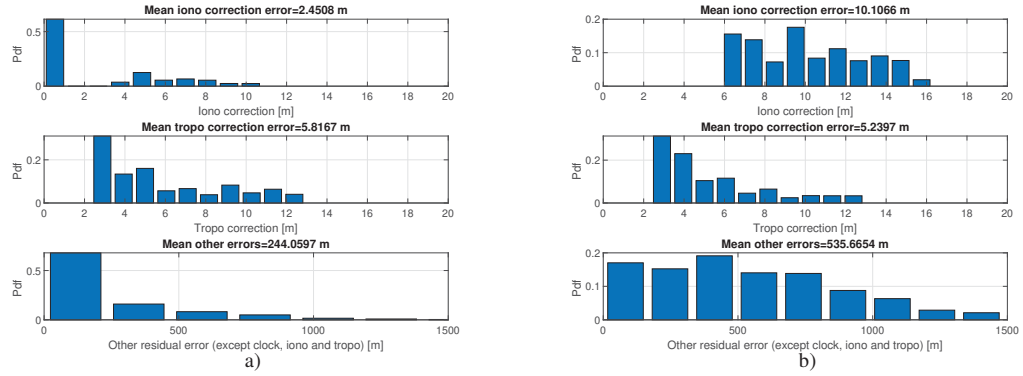

Fig. 9. Atmospheric and multipath error histograms (in absolute values): a) Tecno Spark 7 phone; b) Infinix Hot 6 phone

TABLE IV: VARIATIONS ACROSS MOBILE PHONES, SAME LOCATION IN TOGO, MIXED ENVIRONMENTS: WALK; L1-B1-G1 carrier frequency; GP=GPS, GL=Glonass, BD=Beidou; c= speed of light.

Phone	**Itel w6501**	**Moto E6 play**	**Tecno spark 7**	**Tecno Camon 16 pro**	**Infinix Hot 12i**	**Infinix Hot 6**
Dates	10.3.2023	16.7.2023	26.8.2023	26.8.2023	24.8.2023	27.8.2023
T_{obs} [h]	0.51	0.37	2.54	1.55	0.64	0.61
$GNSS$	$GP\ \ GL$	GL	$GP\ \ GL$	$GP\ \ GL\ \ BD$	$GP\ \ GL\ \ BD$	$GP\ \ GL\ \ BD$
N_{sat}	8.6 4.8	5.8	9.8 6.6	8.0 5.8 7.4	8.7 6.7 7.2	10.2 6.2 5.4
$c\tau_{iono}$ [m]	6.6 6.6	5.1	2.2 1.9	5.5 6.1 6.1	6.2 6.5 6.2	10.2 10.5 9.4
$c\tau_{tropo}$ [m]	5.2 4.9	5.1	5.4 6.6	4.7 5.4 5.2	4.9 5.7 5.0	5.0 5.5 5.7
$c\tau_{other}$ [m]	52.8 168	54.2	245.4 373.9	223.7 201.6 203.2	166.2 126.3 133.1	516.3 606.4 527.4
$Best\ comb.$	GP+GL	GL	GP+GL	GP+GL+BD	GP+GL+BD	GP+GL+BD
ϵ_{2DMean} [m]	5.9	17.7	4.1	2.5	3.1	6.1
ϵ_{2Dstd} [m]	6.8	368.9	11.9	3.2	3.1	6.7
$\epsilon_{z,Mean}$ [m]	9.2	66.4	28.4	25.6	31.7	31.3
$\epsilon_{z,std}$ [m]	13.1	1409.9	50.2	8.4	10.3	5.3

also illustrated in the upper part of Fig. 10, need a power source:

- The water pumps: there are two water pumps, one for filling the tank from water source and the second one serving the dual function of drawing water from the reservoir and pumping it to the activated carbon filter towards the UV/LED module.
- the UV/LED module equipped composed of different LED UV lamps, namely UV-A and UV-C in our currently proposed solutions (see Section IV);
- The standalone satellite-based positioning engine addressed in Section V (used, for example, for route optimization during the access to water or water source detection and geo-tagging, etc.);
- The control board needed to manage the whole system behaviour.

The LEDSOL system is designed to provide 100 litres/day, which corresponds, according to the World Health Organization (WHO), to the amount required to ensure most basic needs of a person. To meet this production capacity, the system must operate at least five times (or cycles) to produce 20L/operating cycle. The total power needs on a daily and yearly basis of LEDSOL system components, as computed by us, are shown in the lower part of Fig. 10: The amount of energy required is estimated at 57 Wh/day, of which 44% is allocated to the UV/LED module, 21% to the system control, 18% to pumping, and the rest is divided between the GNSS 8% and the standby consumption 9%. The average yearly consumption of LEDSOL system is estimated at 21kWh, which, compared for example to an average US household energy consumption per year of 10632 kWh/year, is very small. However, self-powered backpacks commonly found in the market nowadays prioritize the portability and personal use, resulting in their limited voltage range (typically 5V) and modest power output (up to 20W). These specifications cater to various devices and applications that demand mobility, including mobile phones, GNSS systems, tablets, smartphones, power banks, and cameras but cannot meet the criteria of LEDSOL components that work with a voltage of 12V and, as explained above, need a high-power output ($\approx$ 57Wh/day).

B. System constraints and testing results

Based on our studies so far, the chosen design should comply with the following specifications:

- The selected components need to have low electricity consumption attributes, thus operating in DC mode to avoid energy losses due to the DC-to-AC conversion process,
- LEDSOL components must operate with a maximum voltage of 12V, to avoid electrical shocks that might occur with higher voltage in order to ensure the safety of the carrier/worker;
- The use of flexible/foldable solar panels has been adopted for their lightweight and their ease of integration into any design;
- A maximum power point tracking (MPPT) charge controller needs to be used to get the optimum charging power for any given point of time;
- For the energy storage, a lithium-ion battery is to be included in the system due to its advantages (lightweight, few self-discharge, low maintenance and scalability).

One important challenge is to create a system that works under various weather climates (e.g., pilots will be performed in Togo, Romania, and possibly Finland, which have very different weather climates and solar potential). Therefore, simulations can be useful in forecasting the performance of the designed system under a variety of scenarios. We selected PVsyst software to perform such simulations. It is a modelling tool that allows estimating how much solar energy can be gathered from various specific locations, analyze PV losses, and predict system efficiency. Simulation results have been conducted for two selected locations in Algeria (Aïn Tagouraït and Kolea), two selected locations in Togo (Démakpoé and Lomé), one selected location in Romania (Bucharest) one selected location in Finland (Tampere), and the results are shown in Fig. 11 in terms of of collection losses (L_c), system losses (L_s), unused energy (L_u) and produced useful energy per installed kWp/day (Y_f). Moreover, we also defined a Performance Ratio (PR) as the global system efficiency with respect to the nominal installed power and the incident energy and we got the following PR values for the studied locations: 60.53% in Démakpoé, Togo , 60.01% in Lomé, Togo, 56.21% in Aïn Tagouraït, Algeria, 55.71% in Kolea, Algeria, 59.20 % in Bucharest, Romania, and 58.46 % in Tampere, Finland. These show close PV matches in the four studied locations in Africa, but it is to be mentioned that our simulation results indicated that the current PV estimate is undersized in Togo, thus an increase in the capacity of the PV module needs to be considered.

An additional analysis of the losses diagram showed that the system losses are due mainly to the incident global irradiation in the collector plane PV loss due to the radiance level (low-light efficiency); this can be mitigated to some extent by adjusting the tilt angle of the backpack or head basket solution, yet there might be human-derived constraints that could limit this adjustment.

VII. Conclusion

This paper presented the first set of joint results in the three research axes addressed with the EU-funded LEDSOL project: building a novel LED/UV water disinfection unit, implementing standalone low-cost wireless positioning algorithms and developing a solar-powered overall system.

In terms of LED/UV developments, we found out that, on one hand, the quartz window placed in front of the LEDs does not induce a significant attenuation of the UV power. On the other hand, there is significant drop in irradiation level with the distance when measured inside the treatment chamber. This might affect the germicidal action and we need further tests with reference germs such as Escherichia coli (e-coli) in order to assess the prototype's performance.

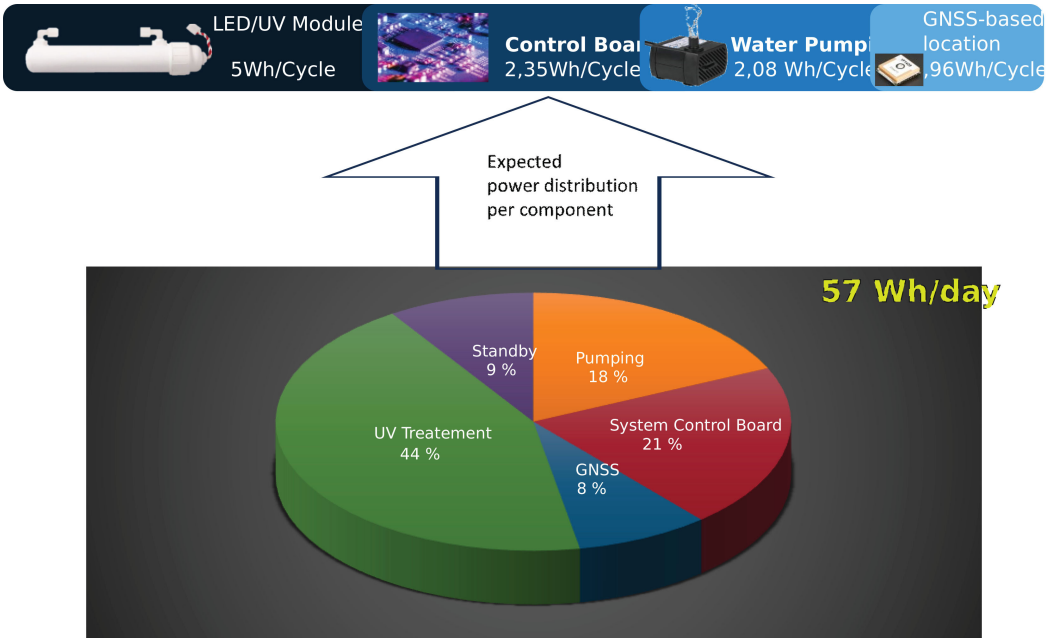

Fig. 10. Distribution of electrical consumption by component and per day

In terms of positioning studies, we found out that moderate positioning accuracy can be achieved with smart consumer devices (Android phones) in standalone modes, where there are no significant fluctuations between the atmospheric models between different phones and locations in Togo, but there are significant variations related to carrier-to-noise ratios (C/N_0), dilution of precision (DOP) metrics and satellite visibility per mobile device. We also found that achievable accuracies are of the order of few meters in horizontal direction, but the altitude (or z-direction) estimate is much more poorer. Surprinsingly, we also found out that Galileo raw data was not supported on any of the Android devices used to collect the GNSS measurements in Togo.

Last but not least, in terms of solar-powered solutions, it was shown that the photovoltaic performance ratios are dependent on the location as well as on the tilting angle of the backpack or head-held basket and that the UV treatment and the control board units are those draining most of the energy of the solar-powered battery.

The next envisaged steps are further testing of UV/LED unit with various microbiological germs, further enhancements of the positioning unit especially in the altitude estimation, and focusing on enhancing the performance ratio of the solar-cell unit.

ACKNOWLEDGMENT

This work has been supported by the LEDSOL project funded within the LEAP-RE programme by the European Union's Horizon 2020 Research and Innovation Program under Grant Agreement 963530, the Academy of Finland grant 352364, the Romanian Ministry of Research, Innovation and Digitization, CNCS/CCCDI - UEFISCDI (project 292 COFUND-LEAP-RE-LEDSOL, within PNCDI III), the Algerian Ministry of Higher Education and Scientific Research (project 31), and the Federal Ministry of Education and Research in Germany. The authors would also like to thank all volunteers who helped in the Android data collection process as well as our international collaborators in LEDSOL project, in addition to the co-authors, from Finland, Togo, Algeria, Romania, and Germany, who provided their valuable insights regarding water-access solutions as well as the field pictures included in this paper.

REFERENCES

[1] "Progress on drinking water, sanitation and hygiene in africa 2000-2020: Five years into the sdgs," United Nations Children's Fund (UNICEF) and World Health Organization (WHO). https://www.unicef.org/wca/reports/progress-drinking-water-sanitation-and-hygiene-africa-2000-2020, 2020.

[2] "Ten causes of the global water crisis," https://concernusa.org/news/global-water-crisis-causes/, last accessed 7.9.2023, 2022.

[3] "United nations world water development report 2023: partnerships and cooperation for water," https://unesdoc.unesco.org/ark:/48223/pf0000384655, last accessed 7.9.2023, 2023.

[4] E. S. Lohan, K. Bierwirth, T. Kodom, M. Ganciu, H. Lebik, R. Elhadi, O. Cramariuc, and I. Mocanu, "Standalone solutions for clean and sustainable water access in africa through smart uv/led disinfection, solar energy utilization, and wireless positioning support," *IEEE Access*, vol. 11, pp. 81 882–81 899, 2023.

[5] J. Rodier, B. Legube, N. Merlet, and et al., *L'analyse de l'eau, eaux naturelles, eaux résiduaires, eau de mer, chimie, physico-chimie, microbiologie, biologie, interprétation des résultats (9th ed.)*. Paris: Dunod, 2009.

[6] C. N. Sawyer and P. L. McCarty, *Chemistry for Sanitary Engineers (2nd ed.)*. New York: McGraw-Hill, 1967.

[7] WHO, "Guidelines for drinking-water quality. 4th edition. geneva, 569 p," Report, 2011.

[8] K. V. Akpataku, M. D. T. Gnazou, T. Y. A. Nomesi, P. Nambo, K. Doni, L. M. Bawa, and G. Djaneye-Boundjou, "Physicochemical and microbiological quality of shallow groundwater in lomé, togo," *Journal*

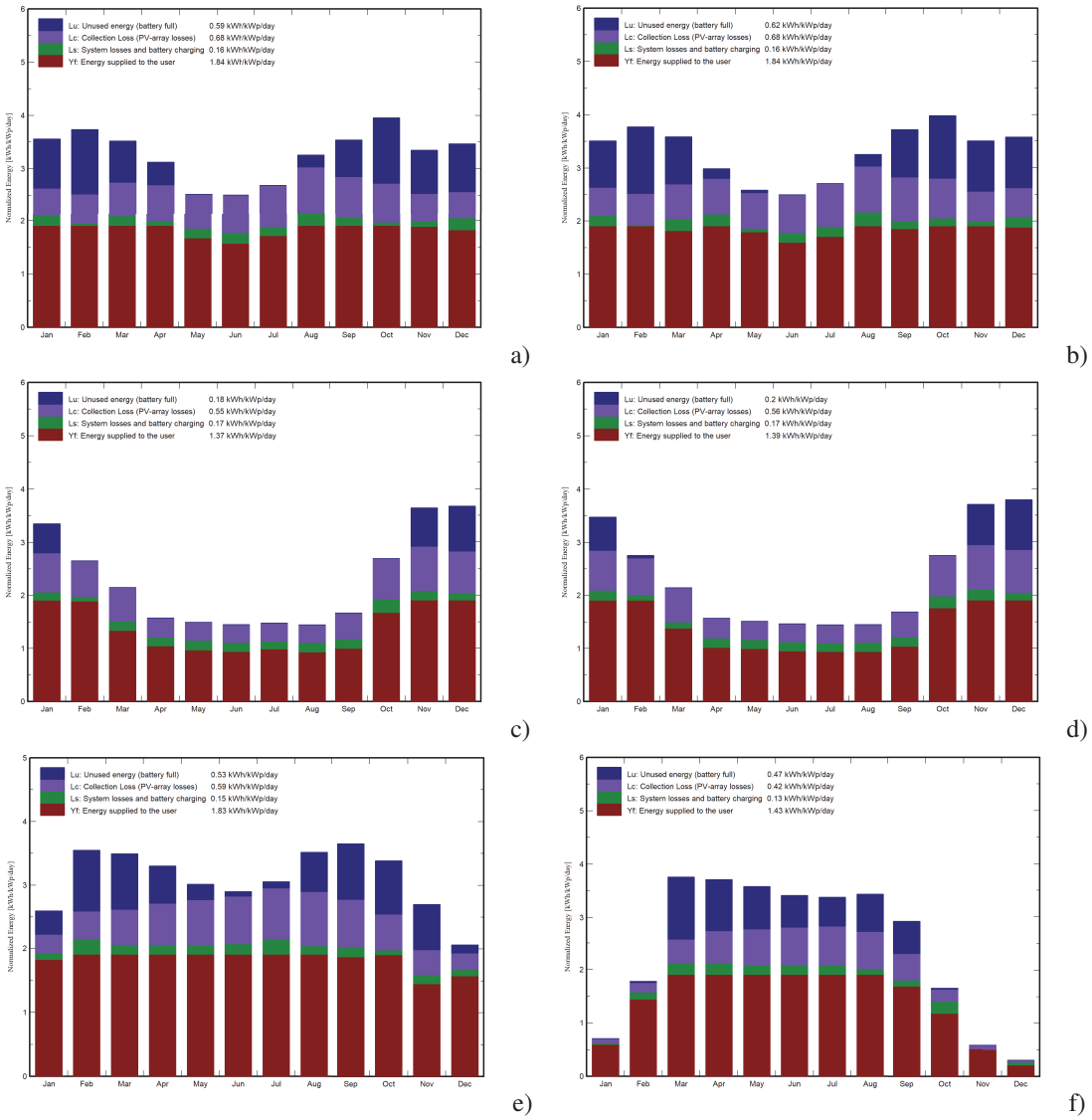

Fig. 11. Photovoltaic analysis results in Africa and Europe; a)Aïn Tagouraït, Algeria, b) Kolea, Algeria, c) Démakpoé, Togo, d) Lomé, Togo, e) Bucharest, Romania and f) Tampere, Finland

of Geoscience and Environment Protection, vol. 08, no. 12, pp. 162–179, 2020. [Online]. Available: https://doi.org/10.4236/gep.2020.812010

[9] "GNSS Raw Measurements Workshop: from research to commercial use," https://www.euspa.europa.eu/newsroom/european-space-expo/gnss-raw-measurements-workshop-research-commercial-use, accessed 12.09.2023, 2018.

[10] P. Crosta and T. Watterton, "Introducing the Galileo PVT App:from Assisted GNSS to NeQuick model in Android," https://shorturl.at/qyDPX, 2018, [Accessed 12-09-2023].

[11] "ESA news - CAMALIOT project launches mobile app for raw GNSS data collection through crowdsourcing," https://shorturl.at/flwEH, accessed 12.09.2023, 2022.

[12] F. Zangenehnejad, Y. Jiang, and Y. Gao, "Gnss observation generation from smartphone android location api: Performance of existing apps,

[13] A. Kuittinen, H. Vesaranta, H. Andersson, P. Jussila, S. Rouhiainen, S. Ruusumaa, S. Gustafsson, and A. Grenier, " MIMIR TAU- an open-source app designed to logged various sensors data in smart issues and improvement," *Sensors*, vol. 23, no. 2, 2023. [Online]. Available: https://www.mdpi.com/1424-8220/23/2/777
devices ," Github [accessed 22.9.2023] https://github.com/agrenier-gnss/MimirTAU, 2023.

[14] "Smartphone-based GNSS Positioning - Today and Tomorrow - Inside GNSS - Global Navigation Satellite Systems Engineering, Policy, and Design — insidegnss.com," Inside GNSS magazine, https://insidegnss.com/smartphone-based-gnss-positioning-today-and-tomorrow/, [Accessed 12-09-2023].

[15] "Ista logger," Munchen University pages, https://www.unibw.de/lrt9/lrt-9.2/forschung/ista-logger/, [Accessed 12-09-2023].

[16] "Google GNSS logger App," https://github.com/google/gps-measurement-tools, accessed 28.04.2023, 2016.

[17] E. D. Kaplan and C. J. Hegarty, *Understanding GPS, Principles and Applications. 3rd Edition*. Artech House, 2017.